CrossMark

RESEARCH ARTICLE

Exploring the Process of Energy Generation in Pathophysiology by Targeted Metabolomics: Performance of a Simple and Quantitative Method

Marta Riera-Borrull,[1,2] Esther Rodríguez-Gallego,[1,2] Anna Hernández-Aguilera,[1,2]
Fedra Luciano,[1,2] Rosa Ras,[3] Elisabet Cuyàs,[4,5] Jordi Camps,[1,2]
Antonio Segura-Carretero,[6,7] Javier A. Menendez,[4,5] Jorge Joven,[1,2]
Salvador Fernández-Arroyo[1,2] (iD)

[1]Unitat de Recerca Biomèdica, Hospital Universitari de Sant Joan, IISPV, Universitat Rovira i Virgili, Reus, Spain
[2]Campus of International Excellence Southern Catalonia, Tarragona, Spain
[3]Center for Omics Sciences, Reus, Spain
[4]Metabolism and Cancer Group, Translational Research Laboratory, Catalan Institute of Oncology (ICO), Girona, Spain
[5]Girona Biomedical Research Institute (IDIBGI), Girona, Spain
[6]Department of Analytical Chemistry, University of Granada, Granada, Spain
[7]Research and Development of Functional Food Centre (CIDAF), Granada, Spain
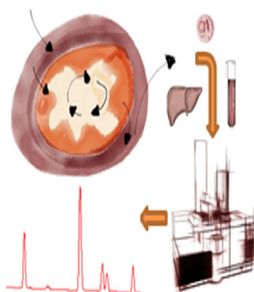
Abstract. Abnormalities in mitochondrial metabolism and regulation of energy balance contribute to human diseases. The consequences of high fat and other nutrient intake, and the resulting acquired mitochondrial dysfunction, are essential to fully understand common disorders, including obesity, cancer, and atherosclerosis. To simultaneously and noninvasively measure and quantify indirect markers of mitochondrial function, we have developed a method based on gas chromatography coupled to quadrupole-time of flight mass spectrometry and an electron ionization interface, and validated the system using plasma from patients with peripheral artery disease, human cancer cells, and mouse tissues. This approach was used to increase sensibility in the measurement of a wide dynamic range and chemical diversity of multiple intermediate metabolites used in energy metabolism. We demonstrate that our targeted metabolomics method allows for quick and accurate identification and quantification of molecules, including the measurement of small yet significant biological changes in experimental samples. The apparently low process variability required for its performance in plasma, cell lysates, and tissues allowed a rapid identification of correlations between interconnected pathways. Our results suggest that delineating the process of energy generation by targeted metabolomics can be a valid surrogate for predicting mitochondrial dysfunction in biological samples. Importantly, when used in plasma, targeted metabolomics should be viewed as a robust and noninvasive source of biomarkers in specific pathophysiological scenarios.
Keywords: Arteriosclerosis, Biomarkers, Cancer, Energy metabolism, Gas chromatography, Mitochondrial dysfunction, Targeted metabolomics

Jorge Joven and Salvador Fernández-Arroyo contributed equally to this work.

Correspondence to: Jorge Joven; *e-mail:* jorge.joven@urv.cat, Salvador Fernández–Arroyo; *e-mail:* sfernandez@fiispv.cat

Introduction

Energy metabolism is the process by which nutrients, such as carbohydrates and fats, are broken down to generate adenosine triphosphate (ATP), the main cellular energy store. A state of energy balance is achieved when energy intake matches expenditure. Deviations from this homeostatic

regulation can result in obesity, where energy intake exceeds demands. Obesity is a pathologic condition that combines inflammatory and metabolic disturbances, which are the immediate cause and/or consequence of many chronic and lethal diseases, including diabetes, atherosclerosis, and cancer [1]. Some of the excess energy is stored as triglyceride in adipose tissue without deleterious effects, but the capacity to store energy is limited and regulated by poorly understood mechanisms. The subsequent excessive accumulation of lipids and other metabolites in tissues that are not designed to manage this condition (e.g., liver, muscle, and pancreas) commonly ensues in an unhealthy course of metabolic events [2, 3]. Detection and treatment of subclinical metabolic derangements are challenging. The clinical picture is difficult to assess because of the combination of multiple and variable stressors such as inflammation, macrophage recruitment, alterations in muscle function, or the chemical composition of the diet. However, the resulting metabolically-related disorders, each with distinct phenotypes, are united by acquired deficiencies in the mitochondrial function and handling of energy [4]. Whether this association is causal or consequential is a matter of debate.

To provide cellular energy, mitochondria use the free energy derived from breakdown of fatty acids and glucose to produce ATP by oxidative phosphorylation. The immediate outcome of deranged energy processing is the reduced ability to switch from one fuel source (e.g., glucose) to another (e.g., fatty acids), resulting in altered flux between glycolytic pathways and oxidative capacity within cells and tissues. The recognition that mitochondria may play a central role in disease has renewed interest in the Randle cycle and the Warburg effect in the pathogenesis of common diseases [5, 6], and may be relevant because the inefficient use of glucose, lipotoxicity, and decreased fat oxidation are key mechanisms to explain most noncommunicable diseases [7, 8]. Consequently, the pharmacologic modulation of mitochondrial function mimicking the effect of exercise and/or caloric restriction may be an attractive therapeutic strategy [9, 10].

In cell-based models, it is relatively simple to assess mitochondrial dynamics, mitophagy (mitochondrial elimination), and pathways aimed to restore and/or maintain mitochondrial function [11, 12]. Assessment in vivo is considerably more challenging and requires sophisticated analytical platforms and stable isotopes to measure metabolites [13, 14]. We recently demonstrated that mitochondrial dysfunction could be assessed in plasma (i.e., noninvasively) using indirect markers of altered cellular energy metabolism [15]. Contrary to the belief that a high-throughput platform for massive metabolite profiling without accurate quantification of each metabolite is the method of choice to provide useful data, we hypothesized that a targeted approach, avoiding the intensive use of bioinformatics and making available actual changes in the concentration of metabolites under different experimental conditions, would be a valuable addition to current analytical tools. To this end, we have designed a simple and rapid method using advances in the technology of gas chromatography coupled to quadrupole time-of-flight mass spectrometry with an electron impact source (GC-EI-QTOF-MS). The method is sensitive for the accurate and simultaneous measurement of organic acids participating in the citric acid cycle (CAC) and selected metabolites representative of the catabolic and anabolic status of several biological systems. We also reasoned that the quantitative exploration of mitochondrial function might rapidly identify correlations between related pathways of metabolism, facilitating the understanding of metabolic conditions. Our results support the usefulness of this technique in in vitro and in vivo settings, and ongoing studies point to a potentially valuable role as a recently available methodology in the search for quantitative biomarkers of disease in epidemiologic cohorts and drug targets to restore cellular energy homeostasis [16–18].

Material and Methods

Chemicals

Methanol (MS grade), methoxyamine hydrochloride (MA), pyridine, *N*-methyl-*N*-(trimethylsilyl)-trifluoroacetamide (TMS) and standards (2-hydroxyglutarate, 3-hydroxybutyrate, 3-phosphoglycerate, 6-phosphogluconate, α-ketoglutarate, acetyl-CoA, aconitate, alanine, aspartic acid, citrate, fructose-1,6-bisphsophate, fructose-6-phosphate, fumarate, glucose, glucose-6-phosphate, glutamate, glutamine, glyceraldehyde-3-phosphate, isoleucine, lactate, leucine, malate, malonyl-coenzyme A, oxaloacetate, phosphoenolpyruvate, pyruvate, ribose-5-phosphate, serine, succinate, and succinyl-coenzyme A and valine) were purchased from Sigma-Aldrich (St. Louis, MO, USA).

Instrumentation

We used a 7890A gas chromatograph coupled with an electron impact source to a 7200 quadrupole time-of-flight mass spectrometer equipped with a 7693 autosampler module and a J&W Scientific HP-5MS column (30 m × 0.25 mm, 0.25 μm) (Agilent Technologies, Santa Clara, CA, USA). Helium was used as a carrier gas at a flow rate of 1.5 mL/min in constant-flow mode. The initial oven temperature was set to 70°C, increased to 190°C at 12°C/min, then raised to 325°C at a rate of 20°C/min and held for 3.25 min. For the MS, ionization was performed using electron impact with a source temperature of 230°C using an electron energy of 70 eV, an emission intensity of 35 μA, and a mass-to-charge range from 70 to 400 *m/z*. The initially selected metabolites to be identified and quantified using this GC-EI-QTOF-MS method are shown in Figure 1, and the selection criteria were based on available knowledge [19].

Isolation and Preparation of Biological Samples

To test the analytical performance and robustness of the method in different biological systems, we used human plasma, cell-culture lysates, and rodent tissues. The procedures used in humans were performed according to protocols approved by our Ethics Committee and Institutional Review Board, and all
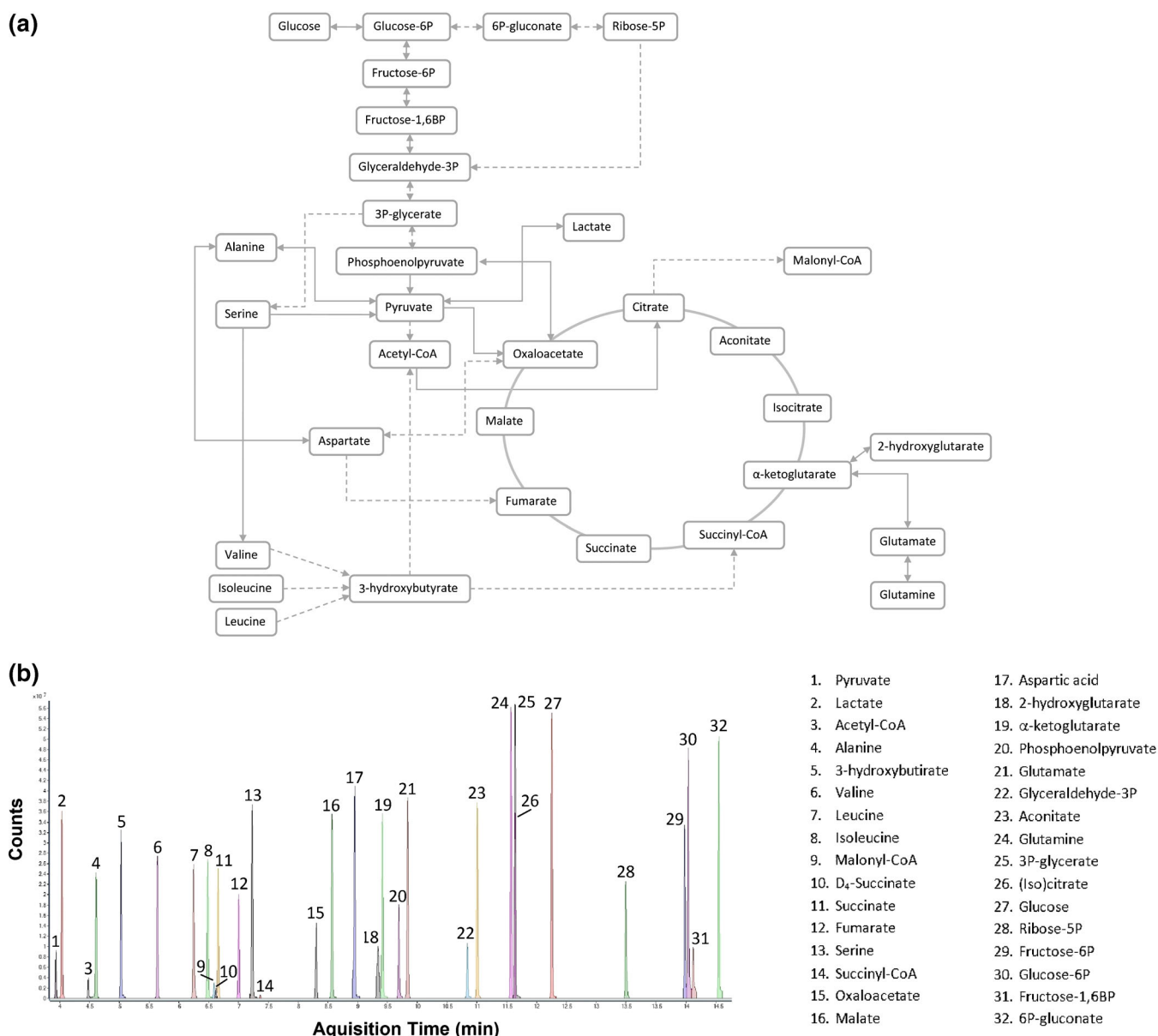
(a)

(b)

1. Pyruvate	17. Aspartic acid
2. Lactate	18. 2-hydroxyglutarate
3. Acetyl-CoA	19. α-ketoglutarate
4. Alanine	20. Phosphoenolpyruvate
5. 3-hydroxybutirate	21. Glutamate
6. Valine	22. Glyceraldehyde-3P
7. Leucine	23. Aconitate
8. Isoleucine	24. Glutamine
9. Malonyl-CoA	25. 3P-glycerate
10. D_4-Succinate	26. (Iso)citrate
11. Succinate	27. Glucose
12. Fumarate	28. Ribose-5P
13. Serine	29. Fructose-6P
14. Succinyl-CoA	30. Glucose-6P
15. Oxaloacetate	31. Fructose-1,6BP
16. Malate	32. 6P-gluconate

Figure 1. (a) Metabolic pathways of measured metabolites involved in energy metabolism. (b) Extracted compound chromatogram (ECC) of the quantifier ion of all metabolites, numbered according to their elution order. ECC was obtained after deconvolution of raw data with a retention time window size factor of 100.00, a signal-to-noise threshold of 2.00 and an absolute area filter of 5000 counts

participants signed an informed consent (EPINOLS 12-03-29/3proj6). Briefly, these included the recruitment of 50 ostensibly healthy participants, aged between 55 and 65 y with an ankle-brachial index (ABI) >0.9, which were body weight- and age-matched with patients presenting intermittent claudication (i.e., peripheral artery disease), ABI <0.9 and staged at grade II according to Fontaine. A sample of blood was drawn from each patient. Participants with diabetes mellitus were excluded to avoid metabolic bias and to limit variability. Further clinical details on the inclusion and exclusion criteria have been previously described [20].

To test the performance of the method in cultured cells, we used MCF10A cells infected with a retroviral KRAS[V12] expression construct, which were generously provided by the

Ben-Ho Park's laboratory and maintained under the previously described culture conditions [21]. Cells were grown to confluence in 6-well plates, then trypsinized and counted (approximately 2×10^6 cells per experiment). We pooled the results obtained in four experiments in triplicate (n = 12).

LDL receptor-deficient (Ldlr^{−/−}) mice develop spontaneous hyperlipidemia and are a useful model for studying atherosclerosis since they present features similar to those observed in the human metabolic syndrome. Mice (C57BL/6J background, The Jackson Laboratory) were housed under standard conditions and given a commercial low fat mouse diet (14% protein rodent maintenance diet; Harlan, Barcelona, Spain). Male mice were sacrificed at 24 wk of age following previously described procedures [22] and tissues (liver and epididymal white

adipose tissue; n = 10 samples, each tissue) were extracted. All procedures were carried out in accordance with institutional guidelines (CEIA, 2014-237).

To ensure high quality data and reduced false discovery rates, a rigorous optimization of pre-analytical steps prior to chromatography was essential. This may vary between laboratories and experimental conditions but includes sample collection, storage, pretreatment and clean-up, as well as software parameters used in data alignment and peak picking. It is particularly important to minimize the time between sample collection and storage at −80°C to less than 1 h to reduce variability. Of note, this method may be used in the quantification of ^{13}C isotopic substrates (data not shown), indicating its suitability for metabolic flux analysis to define the pattern of carbon flow through a metabolic network in cells and tissues [23].

Metabolite Extraction

We investigated different extraction protocols and found that methanol/water (4/1) extraction was efficient for these metabolites. To minimize complexity in the metabolite extraction, we used methanol/water (4/1) mixed with deuterated D_4-succinic acid as surrogate standard (MeOHW-D_4S) to obtain a final concentration of 1 µg/mL. The choice of a unique surrogate standard was considered sufficient as injection quality control and considerably simplifies the procedure. Further, although this method was designed for targeting metabolomics, during experimentations it is not uncommon to require measurement of additional metabolites in the same samples by nuclear magnetic resonance (NMR) or LC/MS. With these procedures, results did not differ significantly using isotopic compounds as internal standard, and there was no need for solvent exchange as previously described [24–26].

Thawed plasma (100 µL) was added to 900 µL of MeOHW-D_4S, vortexed, placed at −20°C for 2 h to precipitate proteins, and centrifuged at 14,000 rpm for 10 min at 4°C to collect the supernatant. As a cautionary note, the use of lower amounts of plasma results in the lack of reliable detection of some metabolites present at low concentrations (e.g., acetyl-CoA or oxaloacetate). Cell pellets were resuspended in 500 µL of MeOHW-D_4S, lysed with three cycles of freezing and thawing using liquid N_2 and sonicated with three cycles of 30 s. Samples were maintained on ice for 1 min between each sonication step. Proteins were precipitated, samples centrifuged, and supernatant collected. Animal tissues (100 mg) were placed in plastic tubes containing 1 mL of MeOHW-D_4S and homogenized using a Precellys 24 system (Izasa, Barcelona, Spain). After centrifugation at 14,000 rpm 10 min at 4°C, supernatant was collected and the homogenization step was repeated. Then proteins were precipitated, samples centrifuged, and supernatant collected. The extraction of nonpolar compounds was performed adding chloroform to have a final proportion of chloroform/methanol (2/1), according to Folch protocol [27]. All supernatants were further vortexed, centrifuged, filtered using 0.22 µm filters, and freeze-dried overnight.

Derivatization

Samples were dried under N_2 and derivatized to rapidly form silyl derivatives. Briefly, in order to protect ketone groups [28], we added 30 µL of methoxylamine hydrochloride dissolved in pyridine [40 mg/mL (0.48 M)] to each sample, which was then incubated for 1.5 h at 37°C with agitation. Then, 45 µL of TMS was added and samples were agitated for 10 min and placed in the dark for 1 h and transferred into a vial before immediate analysis.

Data Analysis

Raw data were processed and compounds were detected and quantified using the Qualitative and Quantitative Analysis B.06.00 software (Agilent Technologies), respectively. Results were compared by one-way ANOVA with Dunnett's multiple pair-wise comparison tests using a significance threshold of 0.05. Other calculations including comparisons with the U of Mann–Whitney test and/or correlations were made using GraphPad Prism software 6.01 (GraphPad Software, San Diego, CA, USA).

Results and Discussion

Method Validation

Calibration curves were obtained for each metabolite by plotting the standard concentration as a function of the peak area. Because the differences in concentration of some metabolites may be highly variable, we required, in some cases, the simultaneous use of different calibration curves covering the expected concentration range for each metabolite. Recovery of each metabolite was calculated and the variation in the percentage of recovery was between 83% and 99%. Ten points of the selected range of all calibration curves were injected and showed linearity with regression coefficients higher than 0.99. The limit of detection (LOD) and quantification (LOQ) for each metabolite were calculated according to International Union of Pure and Applied Chemistry recommendations [29]. Within-day precision or repeatability was calculated injecting each standard on the same day, and between-day repeatability on 5 separate d (n = 5 replicates at three concentration levels) and expressed as relative standard deviation (RSD). Values for each metabolite were considered excellent (RSD from 0.65% to 3.68% and from 1.12 to 4.15%, respectively). Selected and relevant validation parameters are shown in Table 1, and results for other variables may be also examined in Supplemental Table 1.

Table 1. Validation method parameters: regression curve values (slope and intercept), linearity, limit of detection (LOD), limit of quantification (LOQ), intra- and interday % RSD, and recovery (see also Supplemental Table 1)

Metabolite	Slope / intercept	Linearity (R^2)	LOD (μM)	LOQ (μM)	Intraday RSD (%)	Interday RSD (%)	Recovery (%)
2-Hydroxyglutarate	330378 / –64056	0.9991	0.127	0.425	1.12	1.95	91.65
3-Hydroxybutirate	101090 / –15769	0.9976	0.010	0.032	0.65	1.15	96.74
3-Phosphoglycerate	237249 / –2135051	0.9993	0.065	0.215	2.24	3.05	85.65
6-Phospho-gluconate	526980 / –1258050	0.9987 0.9989	0.527	1.758	3.21	3.98	89.35
	87569 / –284587						
α-Ketoglutarate	128155 / 14577	0.9997	0.029	0.098	1.14	2.08	94.99
Acetyl-coenzyme A	10158 / 1785	0.9972	0.610	2.030	1.98	3.01	84.12
Aconitate	749201 / –788502	0.9990	0.010	0.032	2.98	3.65	88.68
Alanine	1987694 / –229517	0.9994	0.288	0.959	1.25	2.34	97.48
Aspartic acid	1715209/ –28378	0.9996	0.835	2.783	0.84	1.25	98.02
(Iso)citrate	1469611 / –271860	0.9996	0.039	0.130	2.54	2.96	93.58
Fructose-1,6-bisphosphate	140842 / –428131	0.9981	0.117	0.389	1.65	2.15	83.26
Fructose-6-phosphate	824733 / –956090	0.9987	0.146	0.487	1.29	1.99	88.69
Fumarate	1119413 / –117375	0.9997	0.040	0.132	0.99	1.34	91.68
Glucose	113676 / –74297	0.9997	0.009	0.029	1.54	2.03	97.35
Glucose-6-phosphate	1040659 / –2961082	0.9990	0.039	0.129	2.14	2.97	96.67
Glutamate	1371976 / –306806	0.9989	0.334	1.114	3.05	4.01	94.31
	284354 / –76489	0.9990					
Glutamine	477954 / –224408	0.9988	0.114	0.380	2.87	3.56	93.11
	957845 / –79154	0.9987					
Glyceraldehyde-3-phosphate	85106 / –44424	0.9979	0.029	0.096	1.32	1.68	87.64
Isoleucine	1652773 / 219943	0.9996	0.108	0.360	0.96	1.42	98.39
Lactate	23667 / 77898	0.9998	0.021	0.070	0.86	1.74	98.96
Leucine	1735828 / 422255	0.9993	0.102	0.340	1.33	1.89	96.84
Malate	336640 / –57888	0.9992	0.113	0.377	0.92	1.12	91.64
Malonyl-coenzyme A	16769 / –359	0.9989	0.039	0.130	2.73	3.06	85.23
Oxaloacetate	70439 / –43811	0.9991	0.590	1.966	3.68	4.15	89.34
Phosphoenolpyruvate	285046 / –222284	0.9981	0.313	1.044	2.38	3.18	92.48
Pyruvate	379309 / 156902	0.9991	0.060	0.200	1.01	1.69	94.67
Ribose-5-phosphate	553740 / –344047	0.9976	0.202	0.675	1.79	2.06	94.58
Serine	1461082 / 11922	0.9999	0.304	1.012	1.14	1.79	97.46
Succinate	176185 / 7109	0.9997	0.077	0.258	0.91	1.35	98.74
Succinyl-coenzyme A	34216 / 5480	0.9998	0.020	0.086	2.06	2.67	87.56
Valine	1836799 / 46946	0.9994	0.098	0.326	1.05	1.68	98.12

Identification and Quantification

The relevant analytical data are summarized in Supplemental Table 2. For some organic acids (3-hydroxybutyrate, fumarate, lactate, oxaloacetate, phosphoenolpyruvate, pyruvate, and succinate) and the internal standard (D_4-succinate), the ion $[M]^+$ was used as qualifier ion and the most abundant ion $[M-CH_3]^+$ resulting from the characteristic loss of a methyl group in TMS after the electron impact, was used as quantifier ion. As shown in Figure 2a, the proposed quantifier ion of acetyl-CoA was observed at *m/z* 219, which is the result of acetate moiety linked to $S–C_2H_4–N–TMS$ from the 4'-phosphopantetheine moiety included in the CoA moiety. The subsequent loss of 15 u suggests the loss of a methyl group from the TMS resulting in an ion at *m/z* 204 that was used as qualifier. For malonyl-CoA, the loss of the TMS from the acid group in malonate moiety linked to S–C2H4–N–TMS from the CoA moiety gives a qualifier ion with *m/z* at 262. The presence of other minor ions with a consecutive loss of 16 u (*m/z* 246 and 230) suggest the loss of the TMS group linked to the acid group of the malonate moiety, which can lose two oxygen atoms consecutively. This is followed by the

loss of the methoxyl group from the methoxyamine, giving an ion at *m/z* 187. To stabilize this ion, a rearrangement is made through a cyclation between the radicals CH2• in malonate moiety and the N• linked to the TMS (Figure 2b). A similar reasoning was used to explain the presence in succinyl-CoA of an ion at *m/z* 276 (qualifier) and minor ions at *m/z* 260 and 244. The N–TMS group and the methyl group from the methoxyamine are finally lost, giving a quantifier ion at *m/z* 174. In this case, to stabilize this structure, the CH_2• radical should be linked to the oxygen from the oxyamine group (Figure 2c). Special attention is required in the identification of phosphate compounds (Figure 2d) because they yield three characteristic fragments [30] and retention time is crucial. Quantifier and qualifier ions used to identify phosphate compounds are summarized in Supplemental Table 2. Of note, with this method isocitrate and citrate have the same retention time. In addition, both give a qualifier ion corresponding to the loss of a carboxyl group and the most abundant ion was $[M-COOTMS-OTMS]^+$ due to the consecutive loss of an OTMS group from the ion ($[M-COOTMS]^+$ (Figure 2e). Although the signal for isocitrate using pure standards is
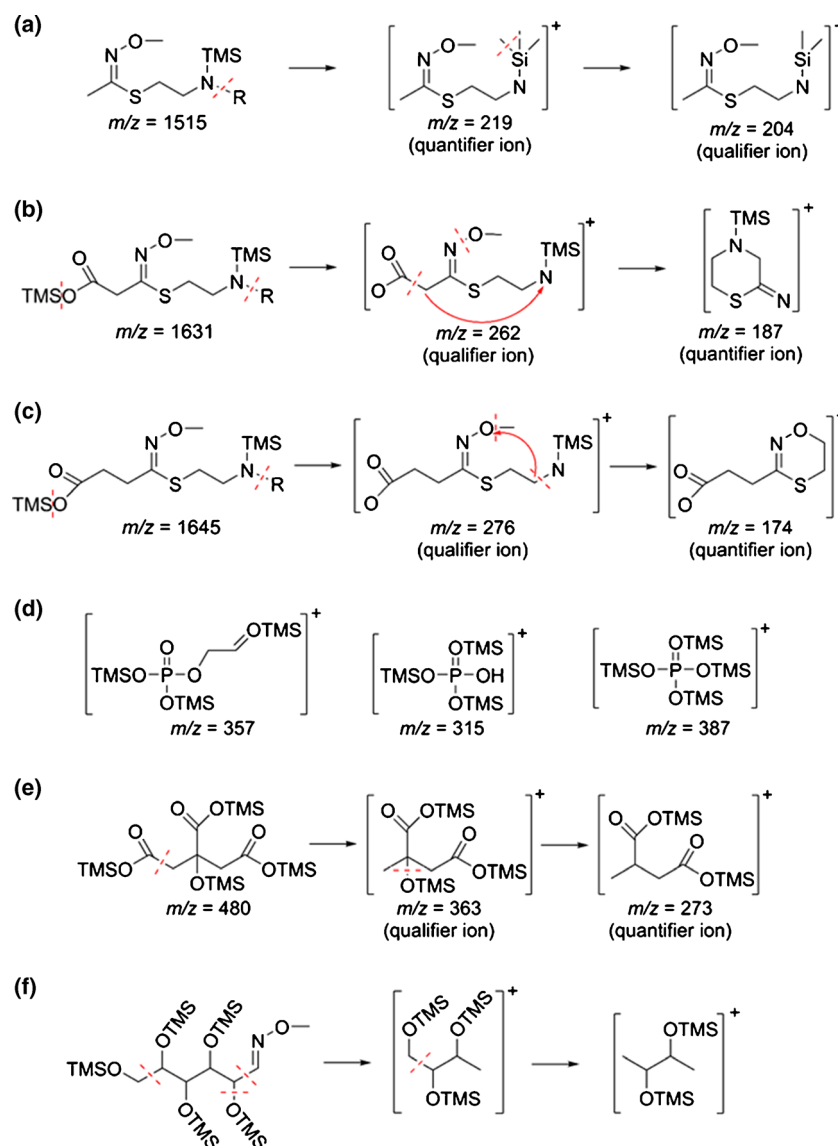
Figure 2. Fragmentation pattern of **(a)** acetyl-CoA, **(b)** malonyl-CoA, **(c)** succinyl-CoA, **(d)** phosphate group, **(e)** (iso)citrate, and **(f)** glucose

significantly less intense, results were expressed as (iso)citrate to denote the lack of chromatographic separation. The quantifier ion for glucose, which is derivatized with five TMS and one MA group (Figure 2f) is $[M-CH_2-CH-NOCH_3-2OTMS]^+$ (attributable to the loss of the methoxyamine group and the CH where it is linked, an OTMS group and a CH_2-OTMS group), and the subsequent loss of an additional CH-OTMS group results in the qualifier ion $[M-CH_2-2CH-NOCH_3-3OTMS]^+$ [31].

In contrast, the interpretation for alanine, valine, leucine, isoleucine, serine, aspartic acid, glutamic acid, malate, and glutamine is simpler because $[M-CH3]^+$ is constant (qualifier ion) and $[M-COOTMS]^+$ is identified as the quantifier ion. $[M-CH_3]^+$, however, was the qualifier ion and $[M-COOTMS]^+$ the quantifier ion for 2-

hydroxyglutarate. Aconitate also shows $[M-CH_3]^+$ as qualifier ion after derivatization with three TMS groups. The loss of two TMS groups and a methyl from the third TMS group yields the quantifier ion $[M-2TMS-CH_3]^+$. Finally, $[M-OCH_3]^+$ (loss of the OCH_3 from the methoxiamine group) is the qualifier ion for α-ketoglutarate, and the additional loss of an OTMS results in the quantifier ion $[M-OCH_3-OTMS]^+$.

Applications in Biological Samples

In our previous efforts with untargeted metabolomics using LC/MS and GC/MS platforms, we found that comparisons between groups were limited by the lack of accurate quantification [32–34]. Conversely, the use of a nuclear magnetic resonance platform [25, 26] provided

Table 2. Metabolite concentrations in plasma (in μM) from selected participants and expressed as mean ± SD. Fold change and significance (P value) are also reported and decimals were set according to the first significant digit of the measured SD

Metabolite	Plasma control (n = 50)	Plasma PAD (n = 50)	Fold change	P value
2-Hydroxyglutarate	9.2 ± 0.4	9.0 ± 0.3	−1.02	N.S.
3-Hydroxybutirate	0.13 ± 0.01	0.31 ± 0.07	2.38	<0.0001
3-Phosphoglycerate	-	-	-	-
6-Phosphogluconate	-	-	-	-
α-Ketoglutarate	3.3 ± 0.2	4.6 ± 0.4	1.39	0.0091
Aconitate	0.52 ± 0.01	4.4 ± 0.9	8.46	<0.0001
Alanine	211 ± 11	203 ± 27	−1.04	N.S.
Aspartic acid	133 ± 3	199 ± 11	1.50	<0.0001
(Iso)citrate	279 ± 13	706 ± 22	2.53	<0.0001
Fructose-1,6-bisphosphate	-	-	-	-
Fructose-6-phosphate	-	-	-	-
Fumarate	0.33 ± 0.02	0.26 ± 0.03	−1.27	<0.0001
Glucose	4856 ± 305	5044 ± 346	1.04	N.S.
Glucose-6-phosphate	N.Q.	N.Q.	-	-
Glutamate	462 ± 366	5197 ± 317	11.25	<0.0001
Glutamine	1115 ± 206	3691 ± 237	3.31	<0.0001
Glyceraldehyde-3-phosphate	-	-	-	-
Isoleucine	49 ± 1	63 ± 2	1.29	<0.0001
Lactate	395 ± 8	359 ± 13	−1.10	0.0323
Leucine	73 ± 2	90 ± 3	1.23	0.0032
Malate	1.57 ± 0.08	3.0 ± 0.3	1.91	<0.0001
Malonyl-coenzyme A	N.Q.	N.Q.	-	-
Oxaloacetate	54 ± 5	N.Q.	-	-
Phosphoenolpyruvate	-	-	-	-
Pyruvate	11 ± 1	10 ± 1	−1.1	0.0270
Ribose-5-phosphate	-	-	-	-
Serine	104 ± 2	145 ± 4	1.39	<0.0001
Succinate	10.7 ± 0.1	12.2 ± 0.4	1.14	N.S.
Succinyl-coenzyme A	6.6 ± 0.9	11.9 ± 0.9	1.80	0.0014
Valine	88 ± 2	105 ± 3	1.19	N.S.

PAD: Peripheral Artery Disease
N.Q.: detected metabolite, but under limit of quantification
N.S.: not significant p-value

excellent reproducibility to quantify certain metabolites but low sensitivity to quantitatively measure the selected metabolites as indirect markers of energy metabolism and mitochondrial function, which included intermediates of glycolysis, the pentose phosphate pathway, branched chain amino acids, and the organic acids of the CAC. We therefore developed the present GC-EI-QTOF-MS analytical platform to measure, after derivatization, these selected compounds, and we found it reliable for use in different biological systems (Tables 2, 3 and 4).

In the first analysis, we compared plasma from healthy controls and patients with stage II peripheral artery disease. Samples injected in triplicate produce RSD values that were similar to those obtained in the precision study. The concentrations of these metabolites have not been previously examined in this condition but metabolites involved in the CAC have been previously suggested as biomarkers of myocardial infarction [35]. Blood was drawn from our patients when they were free of clinical signs of ischemia (i.e., after 1 h of inactivity). Controls with uncompromised circulation in the limb arteries (i.e., ABI > 0.9) had similar cardiovascular risk factors including age, hyperlipidemia, body weight, and current (not past) smoking habit (data not shown). This comparison was designed exclusively for testing

analytical performance in plasma and no clinical implications were intended. Nevertheless, the high concentrations of aconitate, isocitrate, malate, α-ketoglutarate, and succinyl-coenzyme A in patients indicate that mitochondrial function is stimulated rather than inhibited (i.e., contrary to that expected in ischemic conditions) (Table 2). In addition, we found elevated levels of branched chain amino acids, which may also indicate an increased mitochondrial function via their conversion to β-hydroxybutyrate and succinyl-coenzyme A. This may seem paradoxical because elevated levels of branched chain amino acids are usually associated with poor health and cardiovascular disease. One explanation might be the increased endothelial proliferation and accumulation of immune cells resulting in a higher diffusion of these metabolites into the circulation, but may also indirectly point to increased breakdown in the leg muscles [36, 37].

The lack of circulating phosphate compounds was expected considering the hydrophobic nature of the cellular membrane, and it may similarly indicate an absence of significant cellular destruction. Under these conditions, only lactate, which is significantly decreased, may indirectly indicate normal to low glycolytic flux. Also, significant increases of glutamate and glutamine were

Table 3. Metabolite concentration in MCF10A and MCF10A-KRAS^{V12} cells (in μM/mg of protein) expressed as mean ± SD, fold change, and significance (P value). Decimals are reported according to the first significant digit of the measured SD

Metabolite	MCF10A (n = 12)	MCF10A-KRAS^{V12} (n = 12)	Fold change	P value
2-Hydroxyglutarate	-	0.22 ± 0.04	-	-
3-Hydroxybutirate	5.0 ± 0.4	1.78 ± 0.09	−2.81	0.0079
3-Phosphoglycerate	0.28 ± 0.09	36.73 ± 5.13	131.18	<0.0001
6-Phosphogluconate	8.8 ± 1	19.34 ± 2.32	2.20	0.0167
α-Ketoglutarate	0.23 ± 0.08	2.18 ± 0.23	9.48	<0.0001
Aconitate	0.21 ± 0.07	0.14 ± 0.01	−1.50	0.0387
Alanine	65 ± 6	156 ± 21	2.40	0.0067
Aspartic acid	48 ± 6	408 ± 32	8.50	<0.0001
(Iso)citrate	6.3 ± 0.9	5.3 ± 0.6	−1.19	N.S.
Fructose-1,6-bisphosphate	N.Q.	6.4 ± 0.9	-	-
Fructose-6-phosphate	-	N.Q.	-	-
Fumarate	2.4 ± 0.4	10.6 ± 0.6	4.42	<0.0001
Glucose	2.7 ± 0.2	0.22 ± 0.01	−12.27	<0.0001
Glucose-6-phosphate	0.16 ± 0.03	0.64 ± 0.07	4.00	0.0268
Glutamate	10.9 ± 0.6	289 ± 52	26.51	<0.0001
Glutamine	5.8 ± 0.7	5.9 ± 0.7	1.02	N.S.
Glyceraldehyde-3-phosphate	1.6 ± 0.4	1.3 ± 0.4	−1.23	N.S.
Isoleucine	14 ± 2	35 ± 6	2.50	0.0341
Lactate	288 ± 34	812 ± 12	2.82	<0.0001
Leucine	41 ± 8	34 ± 4	−1.21	N.S.
Malate	0.7 ± 0.2	5.0 ± 0.3	7.14	<0.0001
Malonyl-coenzyme A	88 ± 1	40.7 ± 0.6	−2.16	0.0048
Oxaloacetate	-	14 ± 2	-	-
Phosphoenolpyruvate	N.Q.	13 ± 4	-	-
Pyruvate	7 ± 1	94 ± 14	13.43	<0.0001
Ribose-5-phosphate	-	4.9 ± 0.8	-	-
Serine	47 ± 9	48 ± 3	1.02	N.S.
Succinate	12 ± 2	11 ± 2	−1.09	N.S.
Succinyl-coenzyme A	17.3 ± 0.5	31 ± 6	1.79	0.031
Valine	25 ± 2	24 ± 1	−1.04	N.S.

N.Q.: detected metabolite, but under limit of quantification
N.S.: not significant p-value

observed in patients with active atherosclerosis in the limbs, indicating a distinct use of these metabolites in this setting. Our results confirm the validity of our hypothesis with respect to the usefulness of the method to explore the energy metabolism in vivo. These findings may have implications in the search for possible biomarkers and to assess the effectiveness of therapeutic strategies.

We found that the metabolic activity of MCF10A cells engineered to overexpress oncogenic KRAS was significantly higher than MCF10A parental cells under the same culture conditions, strongly suggesting that metabolic reprogramming occurs in breast epithelial cells carrying the constitutively active KRAS^{V12} gene (Table 3). Of note, we were able to detect 2-hydroxyglutarate in MCF10A-KRAS^{V12} cells, which is a product of the mutated isocitrate dehydrogenase and is considered to be an oncometabolite [38]. Further, the increased concentration in some amino acids and indirect markers (ribose-5-phosphate) of metabolic activity in the pentose phosphate pathway were considered as an indication of a higher generation of biomass and endogenous antioxidants in MCF10A-KRAS^{V12} cells to eradicate the reactive oxygen species generated by the accelerated metabolism [39] (Table 3). The increased concentration of glucose-6-phosphate suggests both increased glucose

transport and glycolysis, and indeed lactate production was significantly increased in mutated cells with respect to their isogenic controls. The overall results suggest the dependence on glycolysis for growth, indicative of the Warburg effect. Consequently, our analytical method may be used to perform experiments under different glucose environments and to explore the effect of drugs acting on either glucose uptake or mitochondrial functioning.

We next wished to determine whether this method could be used to explore energy metabolism in a relevant disease model. The simplest approach to test the functionality of the technique was to isolate tissues from mice with different mitochondrial load and importance in energy production. Thus, we compared the concentration of metabolites in adipose tissue and hepatic tissue and found significant differences in the concentration of measured metabolites (Table 4). Some were immediately expected (e.g., amino acids and CAC intermediates). We also found that oxaloacetate and phosphoenolpyruvate were barely detectable in adipose tissue, and the concentration of malonyl-CoA was similar in both tissues. No attempt was made to explore the putative metabolic pathways involved (e.g., lipogenesis), but results show that this method can be used to interrogate metabolic alterations related to excessive energy intake, obesity,

Table 4. Metabolite concentration in mouse tissue samples (in µM/100 mg of tissue) expressed as mean ± SD. Decimals are reported according to the first significant digit of the measured SDThe number of decimals varies according to the concentration

Metabolite	Liver tissue (n = 10)	Adipose tissue (n = 10)
2-Hydroxyglutarate	19 ± 1	0.87 ± 0.09
3-Hydroxybutirate	0.11 ± 0.01	0.064 ± 0.003
3-Phosphoglycerate	18 ± 3	0.24 ± 0.05
6-Phosphogluconate	38206 ± 1648	297 ± 45
α-Ketoglutarate	5.2 ± 0.6	0.15 ± 0.01
Aconitate	47 ± 3	0.061 ± 0.004
Alanine	1663± 188	63 ± 7
Aspartic acid	4259 ± 128	305 ± 59
(Iso)citrate	425 ± 46	31 ± 8
Fructose-1,6-bisphosphate	12 ± 1	1.7 ± 0.4
Fructose-6-phosphate	1323 ± 110	28 ± 3
Fumarate	26 ± 5	0.25 ± 0.04
Glucose	1802 ± 103	249 ± 21
Glucose-6-phosphate	1302 ± 147	191 ± 17
Glutamate	49043 ± 6746	1889 ± 394
Glutamine	2104 ± 273	532 ± 97
Glyceraldehyde-3-phosphate	16 ± 3	0.11 ± 0.05
Isoleucine	730 ± 74	15 ± 3
Lactate	667 ± 47	59 ± 2
Leucine	1009 ± 104	30 ± 6
Malate	319 ± 49	3.8 ± 0.8
Malonyl-coenzyme A	23 ± 2	22 ± 1
Oxaloacetate	2.3 ± 0.3	N.Q.
Phosphoenolpyruvate	12 ± 2	N.Q.
Pyruvate	5.6 ± 0.5	0.32 ± 0.03
Ribose-5-phosphate	470 ± 82	1.7 ± 0.3
Serine	5531 ± 710	182 ± 18
Succinate	138 ± 19	13.1 ± 0.8
Succinyl-coenzyme A	291 ± 7	7.0 ± 0.9
Valine	460 ± 60	22 ± 3

N.Q.: detected metabolite, but under limit of quantification

and the development of associated metabolic dysfunction in the liver (e.g., fatty liver disease).

Method Limitations

This method requires a derivatization procedure, which increases the time used for sample preparation. It should also be considered that the stability of derivatized compounds is limited to a relatively short period of time (not more than 24 h). Although most authors consider citric acid as the only compound found at its time of retention, our efforts to distinguish between isomers were unsuccessful. Finally, because of the low ionization of acetyl-CoA, the concentration in biological samples is not readily detected using GC-MS. To detect this and other possibly useful important metabolites, other analytical platforms are required. Methods using liquid chromatography-mass spectrometry [40–42] are available and provide an accurate approach.

Conclusion

We have developed a simple analytical method using GC-EI-QTOF-MS to separate, detect, and quantify numerous metabolites involved in energy metabolism, including glycolysis, the CAC, and pathways involved in metabolism of lipids, amino acids, and pentose phosphate. This method delivers an overall assessment of metabolism in biological samples used in preclinical and clinical investigation: namely, cell-culture lysates, mouse models of disease, and patient plasma. We have found that GC-EI-QTOF-MS provides better resolution and reproducibility than other available analytical platforms [43] to accurately quantify multiple metabolites. In particular, the measurement of intermediates involved in mitochondrial metabolism, in all likelihood, represents a major advance in the assessment, in vitro, of mitochondrial dysfunction in cells and tissues. The indirect measurement of these intermediates in plasma should be considered as an alternative to assess the mitochondrial dysfunction in vivo for the clinical management of common metabolic diseases.

Acknowledgments

References

1. Kotas, M.E., Medzhitov, R.: Homeostasis, inflammation, and disease susceptibility. Cell 160, 816–827 (2015)
2. Chowdhury, R., Warnakula, S., Kunutsor, S., Crowe, F., Ward, H.A., Johnson, L., Franco, O.H., Butterworth, A.S., Forouhi, N.G., Thompson, S.G., Khaw, K.T., Mozaffarian, D., Danesh, J., Di Angelantonio, E.: Association of dietary, circulating, and supplement fatty acids with coronary risk: a systematic review and meta-analysis. Ann. Intern. Med. 160, 398–406 (2014)
3. Masoodi, M., Kuda, O., Rossmeisl, M., Flachs, P., Kopecky, J.: Lipid signaling in adipose tissue: connecting inflammation and metabolism. Biochim. Biophys. Acta. 1851, 503–518 (2015)
4. Rull, A., Camps, J., Alonso-Villaverde, C., Joven, J.: Insulin resistance, inflammation, and obesity: role of monocyte chemoattractant protein-1 (or CCL2) in the regulation of metabolism. Mediat. Inflamm. 2010, Article ID 326580 (2010)
5. Menendez, J.A., Alarcon, T., Joven, J.: Gerometabolites: the pseudohypoxic aging side of cancer oncometabolites. Cell Cycle 13, 699–709 (2014)
6. Menendez, J.A., Joven, J., Cufi, S., Corominas-Faja, B., Oliveras-Ferraros, C., Cuyas, E., Martín-Castillo, B., López-Bonet, E., Alarcón, T., Vazquez-Martin, A.: The Warburg effect version 2.0: metabolic reprogramming of cancer stem cells. Cell Cycle 12, 1166–1179 (2013)
7. Patergnani, S., Pinton, P.: Mitophagy and mitochondrial balance. Methods Mol. Biol. 1241, 181–194 (2015)
8. Peti-Peterdi, J.: Mitochondrial TCA cycle intermediates regulate body fluid and acid-base balance. J. Clin. Invest. 123, 2788–2790 (2013)
9. Phielix, E., Meex, R., Moonen-Kornips, E., Hesselink, M.K., Schrauwen, P.: Exercise training increases mitochondrial content and ex vivo mitochondrial function similarly in patients with type 2 diabetes and in control individuals. Diabetologia 53, 1714–1721 (2010)
10. Szeto, H.H., James, L.P., Atkinson, A.J.: Mitochondrial pharmacology: its future is now. Clin. Pharmacol. Ther. 96, 629–633 (2014)
11. Divakaruni, A.S., Rogers, G.W., Murphy, A.N.: Measuring mitochondrial function in permeabilized cells using the Seahorse XF analyzer or a Clark-type oxygen electrode. Curr. Protoc. Toxicol. 60, 25.22.21–25.22.16 (2014)
12. Phelan, J.J., MacCarthy, F., Feighery, R., O'Farrell, N.J., Lynam-Lennon, N., Doyle, B., O'Toole, D., Ravi, N., Reynolds, J.V., O'Sullivan, J.: Differential expression of mitochondrial energy metabolism profiles across the

metaplasia-dysplasia-adenocarcinoma disease sequence in Barrett's oesophagus. Cancer Lett. **354**, 122–131 (2014)

13. Abdurrachim, D., Ciapaite, J., Wessels, B., Nabben, M., Luiken, J.J., Nicolay, K., Prompers, J.J.: Cardiac diastolic dysfunction in high-fat diet fed mice is associated with lipotoxicity without impairment of cardiac energetics in vivo. Biochim. Biophys. Acta. **1842**, 1525–1537 (2014)

14. Prompers, J.J., Wessels, B., Kemp, G.J., Nicolay, K.: Mitochondria: investigation of in vivo muscle mitochondrial function by 31P magnetic resonance spectroscopy. Int. J. Biochem. Cell. Biol. **50**, 67–72 (2014)

15. Rodriguez-Gallego, E., Guirro, M., Riera-Borrull, M., Hernandez-Aguilera, A., Marine-Casado, R., Fernandez-Arroyo, S., Beltrán-Debón, R., Sabench, F., Hernández, M., del Castillo, D., Menendez, J.A., Camps, J., Ras, R., Arola, L., Joven, J.: Mapping of the circulating metabolome reveals alpha-ketoglutarate as a predictor of morbid obesity-associated nonalcoholic fatty liver disease. Int. J. Obes. **39**, 279–287 (2015)

16. Floegel, A., Stefan, N., Yu, Z., Muhlenbruch, K., Drogan, D., Joost, H.G., Fritsche, A., Häring, H.U., Hrabě de Angelis, M., Peters, A., Roden, M., Prehn, C., Wang-Sattler, R., Illig, T., Schulze, M.B., Adamski, J., Boeing, H., Pischon, T.: Identification of serum metabolites associated with risk of type 2 diabetes using a targeted metabolomic approach. Diabetes **62**, 639–648 (2013)

17. Inouye, M., Kettunen, J., Soininen, P., Silander, K., Ripatti, S., Kumpula, L.S., Hämäläinen, E., Jousilahti, P., Kangas, A.J., Männistö, S., Savolainen, M.J., Jula, A., Leiviskä, J., Palotie, A., Salomaa, V., Perola, M., Ala-Korpela, M., Peltonen, L.: Metabonomic, transcriptomic, and genomic variation of a population cohort. Mol. Syst. Biol. **6**, 441 (2010)

18. Shah, S.H., Kraus, W.E., Newgard, C.B.: Metabolomic profiling for the identification of novel biomarkers and mechanisms related to common cardiovascular diseases: form and function. Circulation **126**, 1110–1120 (2012)

19. Shin, S.Y., Fauman, E.B., Petersen, A.K., Krumsiek, J., Santos, R., Huang, J., Arnold, M., Erte, I., Forgetta, V., Yang, T.P., Walter, K., Menni, C., Chen, L., Vasquez, L., Valdes, A.M., Hyde, C.L., Wang, V., Ziemek, D., Roberts, P., Xi, L., Grundberg, E.: Multiple TissueHuman Expression Resource (MuTHER) Consortium, Waldenberger, M., Richards, J.B., Mohney, R.P., Milburn, M.V., John, S.L., Trimmer, J., Theis, F.J., Overington, J.P., Suhre, K., Brosnan, M.J., Gieger, C., Kastenmüller, G., Spector, T.D., Soranzo, N.: An atlas of genetic influences on human blood metabolites. Nat. Genet. **46**, 543–550 (2014)

20. Rull, A., Hernandez-Aguilera, A., Fibla, M., Sepulveda, J., Rodriguez-Gallego, E., Riera-Borrull, M., Sirvent, J.J., Martín-Paredero, V., Menendez, J.A., Camps, J., Joven, J.: Understanding the role of circulating chemokine (C–C motif) ligand 2 in patients with chronic ischemia threatening the lower extremities. Vasc. Med. **19**, 442–451 (2014)

21. Konishi, H., Karakas, B., Abukhdeir, A.M., Lauring, J., Gustin, J.P., Garay, J.P., Konishi, Y., Gallmeier, E., Bachman, K.E., Park, B.H.: Knock-in of mutant K-ras in nontumorigenic human epithelial cells as a new model for studying K-ras mediated transformation. Cancer Res. **67**, 8460–8467 (2007)

22. Joven, J., Rull, A., Ferre, N., Escola-Gil, J.C., Marsillach, J., Coll, B., Alonso-Villaverde, C., Aragones, G., Claria, J., Camps, J.: The results in rodent models of atherosclerosis are not interchangeable: the influence of diet and strain. Atherosclerosis **195**, e85–e92 (2007)

23. Sauer, U.: Metabolic networks in motion: 13C-based flux analysis. Mol. Syst. Biol. **2**, 62 (2006)

24. Beltran, A., Suarez, M., Rodriguez, M.A., Vinaixa, M., Samino, S., Arola, L., Correig, X., Yanes, O.: Assessment of compatibility between extraction methods for NMR- and LC/MS-based metabolomics. Anal. Chem. **84**, 5838–5844 (2012)

25. Rull, A., Vinaixa, M., Angel Rodriguez, M., Beltran, R., Brezmes, J., Canellas, N., Correig, X., Joven, J.: Metabolic phenotyping of genetically modified mice: an NMR metabonomic approach. Biochimie. **91**, 1053–1057 (2009)

26. Vinaixa, M., Rodriguez, M.A., Rull, A., Beltran, R., Blade, C., Brezmes, J., Correig, X., Joven, J.: Metabolomic assessment of the effect of dietary cholesterol in the progressive development of fatty liver disease. J. Proteome. Res. **9**, 2527–2538 (2010)

27. Folch, J., Lees, M., Sloane Stanley, G.H.: A simple method for the isolation and purification of total lipides from animal tissues. J. Biol. Chem. **226**, 497–509 (1957)

28. Yang, L., Kombu, R.S., Kasumov, T., Zhu, S.H., Cendrowski, A.V., David, F.: Metabolomic and mass isotopomer analysis of liver gluconeogenesis and citric acid cycle. I. Interrelation between gluconeogenesis and cataplerosis; formation of methoxamates from aminooxyacetate and ketoacids. J. Biol. Chem. **283**, 21978–21987 (2008)

29. Currie, L.A.: Nomenclature in evaluation of analytical methods including detection and quantification capabilities (IUPAC Recommendations 1995). Anal. Chim. Acta. **391**, 105–126 (1999)

30. Wegner, A., Weindl, D., Jager, C., Sapcariu, S.C., Dong, X., Stephanopoulos, G., Hiller, K.: Fragment formula calculator (FFC): determination of chemical formulas for fragment ions in mass spectrometric data. Anal. Chem. **86**, 2221–2228 (2014)

31. Sakamoto, Y., Nakagawa, K., Miyagawa, H., Kawana, S., Fukumoto, S.: Quantitative analysis of stable isotopes of glucose in blood plasma using quadrupole GC-MS. Shimadzu Corporation, GC-MS technical repport No. 2 (2010)

32. Garcia-Heredia, A., Kensicki, E., Mohney, R.P., Rull, A., Triguero, I., Marsillach, J., Tormos, C., Mackness, B., Mackness, M., Shih, D.M., Pedro-Botet, J., Joven, J., Sáez, G., Camps, J.: Paraoxonase-1 deficiency is associated with severe liver steatosis in mice fed a high-fat high-cholesterol diet: a metabolomic approach. J. Proteome. Res. **12**, 1946–1955 (2013)

33. Holvoet, P., Rull, A., Garcia-Heredia, A., Lopez-Sanroma, S., Geeraert, B., Joven, J., Camps, J.: Stevia-derived compounds attenuate the toxic effects of ectopic lipid accumulation in the liver of obese mice: a transcriptomic and metabolomic study. Food Chem. Toxicol. **77**, 22–33 (2015)

34. Rull, A., Geeraert, B., Aragones, G., Beltran-Debon, R., Rodriguez-Gallego, E., Garcia-Heredia, A., Pedro-Botet, J., Joven, J., Holvoet, P., Camps, J.: Rosiglitazone and fenofibrate exacerbate liver steatosis in a mouse model of obesity and hyperlipidemia. A transcriptomic and metabolomic study. J. Proteome. Res. **13**, 1731–1743 (2014)

35. Yao, H., Shi, P., Zhang, L., Fan, X., Shao, Q., Cheng, Y.: Untargeted metabolic profiling reveals potential biomarkers in myocardial infarction and its application. Mol. Biosyst. **6**, 1061–1070 (2010)

36. Greenhaff, P.L., Karagounis, L.G., Peirce, N., Simpson, E.J., Hazell, M., Layfield, R., Wackerhage, H., Smith, K., Atherton, P., Selby, A., Rennie, M.J.: Disassociation between the effects of amino acids and insulin on signaling, ubiquitin ligases, and protein turnover in human muscle. Am. J. Physiol. Endocrinol. Metab. **295**, E595–E604 (2008)

37. Suhre, K., Meisinger, C., Doring, A., Altmaier, E., Belcredi, P., Gieger, C., Chang, D., Milburn, M.V., Gall, W.E., Weinberger, K.M., Mewes, H.W., Hrabé de Angelis, M., Wichmann, H.E., Kronenberg, F., Adamski, J., Illig, T.: Metabolic footprint of diabetes: a multiplatform metabolomics study in an epidemiological setting. PLoS ONE **5**, e13953 (2010)

38. Krell, D., Mulholland, P., Frampton, A.E., Krell, J., Stebbing, J., Bardella, C.: IDH mutations in tumorigenesis and their potential role as novel therapeutic targets. Future Oncol. **9**, 1923–1935 (2013)

39. Chen, X., Qian, Y., Wu, S.: The Warburg effect: evolving interpretations of an established concept. Free Radic. Biol. Med. **79**, 253–263 (2015)

40. Armando, J.W., Boghigian, B.A., Pfeifer, B.A.: LC-MS/MS quantification of short-chain acyl-CoA's in *Escherichia coli* demonstrates versatile propionyl-CoA synthetase substrate specificity. Lett. Appl. Microbiol. **54**, 140–148 (2012)

41. Gilibili, R.R., Kandaswamy, M., Sharma, K., Giri, S., Rajagopal, S., Mullangi, R.: Development and validation of a highly sensitive LC-MS/MS method for simultaneous quantitation of acetyl-CoA and malonyl-CoA in animal tissues. Biomed. Chromatogr. **25**, 1352–1359 (2011)

42. Hayashi, O., Satoh, K.: Determination of acetyl-CoA and malonyl-CoA in germinating rice seeds using the LC-MS/MS technique. Biosci. Biotechnol. Biochem. **70**, 2676–2681 (2006)

43. Lei, Z., Huhman, D.V., Sumner, L.W.: Mass spectrometry strategies in metabolomics. J. Biol. Chem. **286**, 25435–25442 (2011)